PHYSICAL REVIEW B **74**, 113104 (2006)

Electronic structures of layered perovskite Sr_2MO_4 (M=Ru, Rh, and Ir)

S. J. Moon,[1] M. W. Kim,[1] K. W. Kim,[1] Y. S. Lee,[2] J.-Y. Kim,[3] J.-H. Park,[3,4] B. J. Kim,[5] S.-J. Oh,[5] S. Nakatsuji,[6] Y. Maeno,[6] I. Nagai,[7] S. I. Ikeda,[7] G. Cao,[8] and T. W. Noh[1,*]
[1]*ReCOE & FPRD, School of Physics and Astronomy, Seoul National University, Seoul 151-747, Korea*
[2]*Department of Physics, Soongsil University, Seoul 156-743, Korea*
[3]*Pohang Accelerator Laboratory, Postech, Pohang 790-784, Korea*
[4]*Department of Physics & Electron Spin Science Center, Postech, Pohang 790-784, Korea*
[5]*CSCMR & FPRD, School of Physics and Astronomy, Seoul National University, Seoul 151-747, Korea*
[6]*Department of Physics, Kyoto University, Kyoto 606-8501, Japan*
[7]*National Institute of Advanced Industrial Science and Technology, Tsukuba, Ibaraki 305-8568, Japan*
[8]*Department of Physics and Astronomy, University of Kentucky, Lexington, Kentucky 40506, USA*
(Received 30 June 2006; published 13 September 2006)

We investigated the electronic structures of the two-dimensional layered perovskite Sr_2MO_4 (M=4d Ru, 4d Rh, and 5d Ir) using optical spectroscopy and polarization-dependent O 1s x-ray absorption spectroscopy. While the ground states of the series of compounds are rather different, their optical conductivity spectra $\sigma(\omega)$ exhibit similar interband transitions, indicative of the common electronic structures of the 4d and 5d layered oxides. The energy splittings between the two e_g orbitals, i.e., $d_{3z^2-r^2}$ and $d_{x^2-y^2}$, are about 2 eV, which is much larger than those in the pseudocubic and 3d layered perovskite oxides. The electronic properties of the Sr_2MO_4 compounds are discussed in terms of the crystal structure and the extended character of the 4d and 5d orbitals.

DOI: 10.1103/PhysRevB.74.113104 PACS number(s): 71.20.−b, 78.20.−e, 78.70.Dm

Transition metal oxides (TMOs) with layered perovskite structures have attracted much attention due to their exotic physical properties, such as high-T_c superconductivity in cuprates,[1] one-dimensional charge and spin self-organization in nickelates,[2] and charge and orbital ordering in manganites.[3] These phenomena in 3d TMOs originate from the low dimensionality and the related anisotropy in the electronic structure, as well as generic correlation effects in the d orbitals. The discovery of unconventional superconductivity in 4d layered Sr_2RuO_4 has initiated intense interest in 4d and 5d layered compounds because of the potential to discover novel phenomena.[4]

The electronic structures of 4d and 5d layered TMOs should be quite different from those of 3d TMOs. For a 3d TMOs, the Hund coupling energy J_H ($\sim$3 eV) is much larger than the crystal field splitting 10Dq (1–2 eV) between the t_{2g} and e_g states.[5,6] For example, the electronic structure of $LaSrMnO_4$ (3d^4 system) with a high-spin configuration is drawn schematically in Fig. 1(a).[5,6] The exchange splitting of the e_g states is sufficiently large to place the $e_g^{\uparrow}$ band below the $t_{2g}^{\downarrow}$ band. The elongation of MnO_6 octahedra results in energy splitting between the two e_g states (i.e., $d_{3z^2-r^2}$ and $d_{x^2-y^2}$), and this value is typically about 1 eV. Since most interband transitions are very broad, this e_g orbital splitting is barely observed in the optical conductivity spectra $\sigma(\omega)$. In contrast, for 4d and 5d TMOs, the crystal field splitting should be larger than the exchange splitting due to the extended nature of the 4d and 5d orbitals. Therefore, they are usually in the low-spin configuration, in which all of the t_{2g} bands are lower than the e_g bands. According to recent x-ray absorption spectroscopy (XAS) studies on the $Ca_{2-x}Sr_xRuO_4$ system, the energy splitting between $d_{3z^2-r^2}$ and $d_{x^2-y^2}$ is sizable, while the exchange splitting in the e_g state is not detectable, as shown in Fig. 1(b).[7] (The e_g orbital splitting between $d_{3z^2-r^2}$ and $d_{x^2-y^2}$ was reported to be about 3 eV, which is quite unusual. To the best of our knowledge, large e_g orbital splitting has not been reported in any other compound.)

To attain further insights into the electronic structure of 4d and 5d layered compounds, we made systematic studies of Sr_2MO_4 (M=Ru, Rh, and Ir). Each Sr_2MO_4 has the layered perovskite structure. The space group symmetry of Sr_2RuO_4 is $I4/mmm$, and the Ru-O-Ru bond angle is 180°.[8] In Sr_2RhO_4 and Sr_2IrO_4, the MO_6 octahedra are rotated with respect to the c axis, so their space group symmetry becomes $I4_1/acd$.[9,10] The d-orbital configurations of the Ru^{4+}, Rh^{4+}, and Ir^{4+} ions are 4d^4, 4d^5, and 5d^5, respectively. Despite having a similar crystal structure, their electronic ground states differ somewhat. While Sr_2RuO_4 is a superconductor below about 1 K, the paramagnetic metallic state of Sr_2RhO_4 is retained to 36 mK.[11] Interestingly, Sr_2IrO_4 is an insulator with a canted ferromagnetic ordering.[10]

In this paper we report the optical conductivity spectra $\sigma(\omega)$ and polarization-dependent O 1s XAS data for Sr_2MO_4 (M=Ru, Rh, and Ir). The optical spectra showed three charge transfer transitions in the energy region between 0 and 8 eV with a systematic trend with M. By comparing $\sigma(\omega)$ with the XAS spectra, we could determine the electronic structures of Sr_2MO_4. In particular, we found that the splitting of the e_g orbitals due to the elongation of the MO_6 octahedra along the c axis is quite large, about 2 eV. We also discuss the low-energy optical responses of Sr_2MO_4 in relation to their ground states.

Single crystals of Sr_2RuO_4 and Sr_2RhO_4 were grown using the floating zone method,[4,11] and the Sr_2IrO_4 single-crystalline sample was grown using flux technique.[10] The magnetic and transport properties of $Sr_2RhO_{4-\delta}$ depend on its oxygen content.[11] We used stoichiometric $Sr_2RhO_{4.00}$ for our measurements. We measured the ab-plane reflectivity spectra $R(\omega)$ at room temperature over a wide photon energy region between 5 meV and 30 eV. The corresponding $\sigma(\omega)$

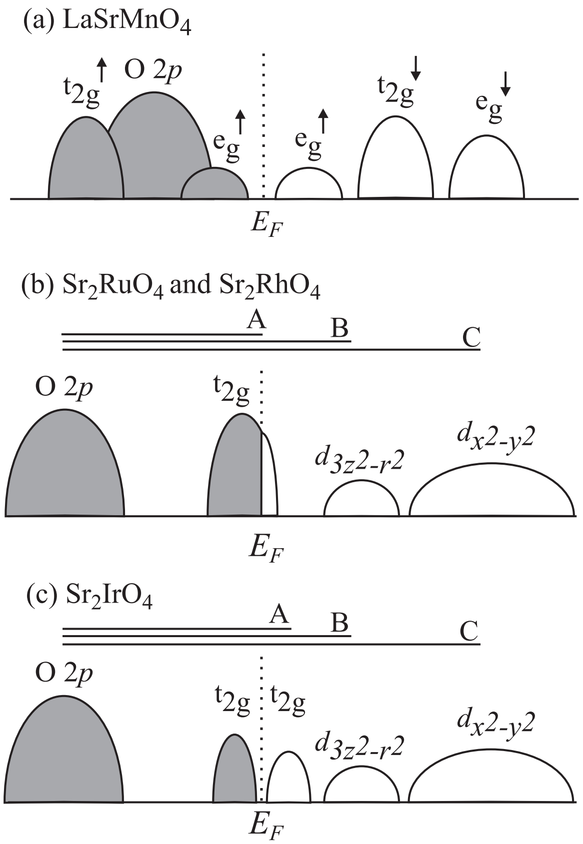

FIG. 1. Schematic diagrams of the electronic structures of (a) LaSrMnO$_4$, (b) Sr$_2$RuO$_4$ and Sr$_2$RhO$_4$, and (c) Sr$_2$IrO$_4$. E_F represents the Fermi level. The arrows pointing up and down indicate spin up and spin down, respectively. The schematic diagram of the electronic structure of LaSrMnO$_4$ is drawn based on Ref. 5.

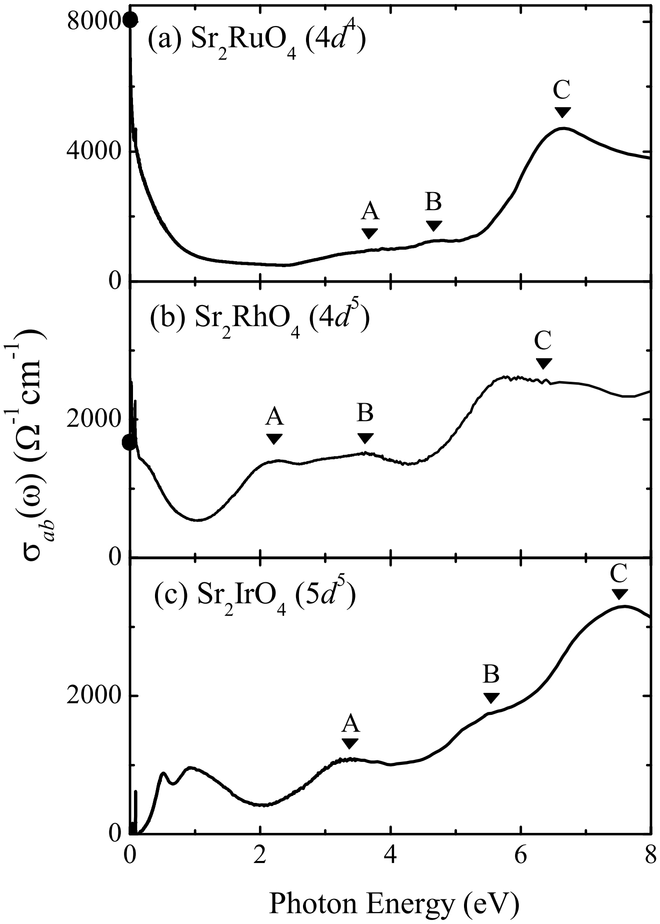

FIG. 2. The ab-plane $\sigma(\omega)$ of (a) Sr$_2$RuO$_4$, (b) Sr$_2$RhO$_4$, and (c) Sr$_2$IrO$_4$ at room temperature. The solid triangles and letters represent the optical transitions, which are shown in Fig. 1. The solid circles are the dc conductivities of Sr$_2$RuO$_4$ and Sr$_2$RhO$_4$ at room temperature (Refs. 11 and 12).

were obtained using the Kramers-Kronig (KK) transformation of $R(\omega)$. We checked the validity of our KK analysis by measuring $\sigma(\omega)$ between 0.6 and 6.4 eV independently using spectroscopic ellipsometry.

Figure 2 shows the ab-plane $\sigma(\omega)$ of Sr$_2$RuO$_4$, Sr$_2$RhO$_4$, and Sr$_2$IrO$_4$. First, we will focus on the optical transitions above 1.5 eV. As shown in Fig. 2, the $\sigma(\omega)$ of Sr$_2$RuO$_4$, Sr$_2$RhO$_4$, and Sr$_2$IrO$_4$ all showed three interband transitions. According to the literature on regular perovskite TMOs, the optical transitions from the O 2p to Sr d bands are usually located at about 9–10 eV.[13,14] Therefore, all of the A, B, and C peaks observed in Fig. 2 might come from the charge transfer transition from O 2p to M d bands.

Polarization-dependent O 1s XAS spectra of Sr$_2$RuO$_4$ have already been reported. To obtain further insights, we measured O 1s XAS spectra of Sr$_2$RhO$_4$ and Sr$_2$IrO$_4$ at the EPU6 beamline of the Pohang Light Source (PLS). O 1s XAS detects the transition from O 1s to O 2p orbitals. The XAS measurements can probe the unoccupied density of states that are strongly hybridized with the O 2p orbitals. With the incident E vector mainly in plane (i.e., $\theta=0°$), the XAS spectra should show only the M d orbital states that are strongly coupled with O $2p_{x/y}$. With $\theta=60°$, the XAS spectra should show the M d orbital states coupled with both O $2p_{x/y}$ and O $2p_z$, but the latter states should make a larger contribution. The polarization dependence should be large, since the d orbitals have strong directional dependence. The main bondings of the in-plane O $2p_{x/y}$ orbitals are O $2p_{x/y}-d_{xy}$ (xy_P) and O $2p_{x/y}$-$d_{x^2-y^2}$ ($x^2-y_P^2$), and that of the apical O $2p_{x/y}$ orbitals is O $2p_{x/y}$-$d_{yz/zx}$ (yz/zx_A), while those of the in-plane and apical O $2p_z$ orbitals are O $2p_z$-$d_{yz/zx}$ (yz/zx_P) and O $2p_z$-$d_{3z^2-r^2}$ (z_A^2), respectively. The $d_{3z^2-r^2}$ orbital mainly bonds with the apical O $2p_z$, but still bonds weakly with the in-plane O $2p_{x/y}$ (z_P^2). Therefore, the spectra with $\theta=0°$ should show the contributions of the xy_P, $x^2-y_P^2$, yz/zx_A, and z_P^2 states, while the yz/zx_P and z_A^2 states should contribute more strongly in the spectra with $\theta=60°$.

Figure 3 shows the polarization-dependent XAS spectra of Sr$_2M$O$_4$. [The XAS spectrum of Sr$_2$RuO$_4$ (Ref. 7) is included in Fig. 3(a) for better comparison with those of other compounds.] All three compounds exhibit very similar XAS spectra with strong polarization dependence. Considering the directional dependence of the p-d hybridization, the four peaks in the $\theta=0°$ spectra can be assigned as yz/zx_A, xy_P, z_P^2, and $x^2-y_P^2$, and the two peaks in the $\theta=60°$ spectra can be assigned as yz/zx_P and z_A^2 from the lowest energy. In the layered TMOs, the core-hole energy of the apical oxygen is

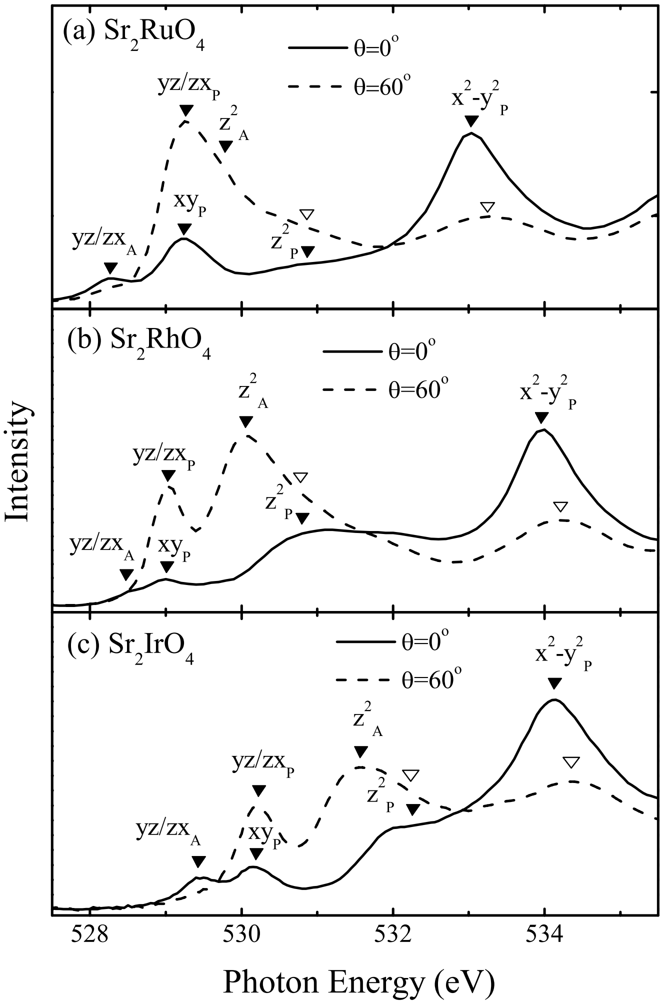

FIG. 3. Polarization-dependent O 1*s* XAS spectra of (a) Sr_2RuO_4, (b) Sr_2RhO_4, and (c) Sr_2IrO_4. The spectra of Sr_2RuO_4 are taken from Ref. 7. θ is the incidence angle of light to the surface normal. The solid triangles and labels represent the positions and characters of empty *d* bands, respectively. The open triangles indicate z_P^2 and $x^2-y_P^2$ states, which are shown in the $\theta=60°$ spectrum due to the partial in-plane polarization of incident light.

lower than that of the in-plane oxygen due to the difference in the chemical environment.[7] Therefore, the t_{2g} states related to the apical oxygen (yz/zx_A) should have lower energy than those related to the in-plane oxygen (xy_P), which is also the case for the e_g orbitals (z_A^2 and z_P^2).

These peak assignments in the XAS spectra are also consistent with those of $\sigma(\omega)$ obtained from the optical measurements. From the XAS results, three *p*-*d* charge transfer transitions are predicted to be observed in the $\sigma(\omega)$: those from O 2*p* to $d_{xy/yz/zx}$ (peak *A*), $d_{3z^2-r^2}$ (peak *B*), and $d_{x^2-y^2}$ (peak *C*) from the lowest energy. This is well reproduced in $\sigma(\omega)$ as shown in Fig. 2. Using the Lorentz oscillators, we estimated the peak positions of the interband transitions to be about 3.7, 4.7, and 6.7 eV for Sr_2RuO_4, about 2.2, 3.6, and 6.3 eV for Sr_2RhO_4, and about 3.3, 5.4, and 7.5 eV for Sr_2IrO_4. We summarized the peak positions in $\sigma(\omega)$ and the XAS spectra in Fig. 4. It is clear that the two independently determined peak positions are quite consistent, which indicates the self-consistency of our assignments.

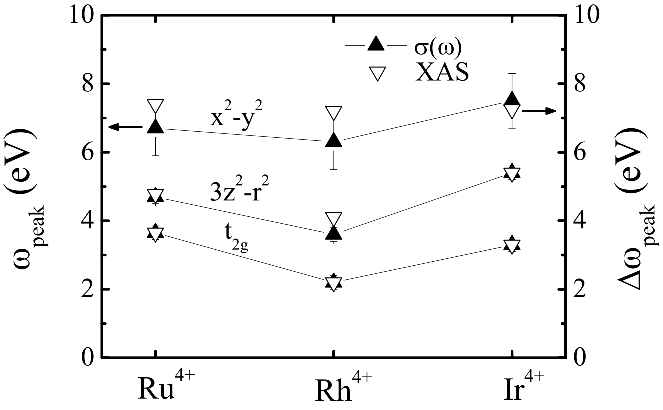

FIG. 4. The peak positions of the interband transitions in $\sigma(\omega)$ and relative peak positions of the XAS spectra of Sr_2MO_4. In order to compare two spectra, we shifted the energy values of the empty t_{2g} states in the XAS spectra to the values of the corresponding optical transitions: O $2p \rightarrow M$ t_{2g}.

It is interesting to examine the change in the charge transfer energies in the Sr_2MO_4 series with *M*. As shown in Fig. 4, the charge transfer peaks of Sr_2RhO_4 have the lowest values in the series. This change with *M* could be explained by the ionic model, which has been applied to explain the electronic structures of numerous 3*d* TMOs.[15,16] According to the ionic model, the charge transfer energy decreases, as the ionization energy of a transition metal increases. For a given oxidation state, the ionization energy of a transition metal increases with the atomic number and decreasing principal quantum number. Therefore, the charge transfer energies of Sr_2RhO_4 should be the smallest in our Sr_2MO_4 series. In this respect, the systematic changes in the charge transfer energies in our 4*d* and 5*d* layered oxides can be explained in terms of the ionic model.

It is unexpected that the energy splittings of the $d_{3z^2-r^2}$ and $d_{x^2-y^2}$ orbitals for Sr_2RhO_4 and Sr_2IrO_4 are quite large, i.e., ~2 eV, like Sr_2RuO_4. These e_g orbital splittings have not been observed in pseudocubic perovskite 4*d* $SrMO_3$, which have nearly undistorted MO_6 octahedra.[14] For the layered Sr_2MO_4 compounds, the MO_6 octahedra are elongated along the *c* axis.[8–10] It is believed that t_{2g} and the e_g orbitals split in such a way that the energy of the d_{xy} and $d_{x^2-y^2}$ orbitals is higher than that of $d_{yz/zx}$ and $d_{3z^2-r^2}$, respectively. This simple idea appears to agree with our finding that the e_g orbital splitting becomes rather large (~2 eV), while that of the t_{2g} states is negligible. Indeed, the energy splitting of the t_{2g} states in Ca_2RuO_4 should be only 0.2 eV.[17,18] Since the hybridization of the O 2*p* orbitals should be stronger with the e_g than the t_{2g} orbitals, the energy states of the e_g orbitals could be more sensitive to lattice distortion, which can lead to larger e_g orbital splitting. Further investigations of the large e_g orbital splitting in other 4*d* and 5*d* layered materials are warranted.

Compared to our 4*d* and 5*d* layered compounds, the reported values of the e_g orbital splittings for 3*d* layered TMOs are much smaller. XAS measurement of the layered manganite $La_{2-2x}Sr_{1+2x}Mn_2O_7$ has revealed that the corresponding energy splitting is about 0.4 eV.[19] The XAS measurement of the layered nickelate $La_{2-x}Sr_xNiO_4$ also shows an e_g orbital splitting of about 0.7 eV.[20] This implies that the electron-lattice couplings of the 4*d* and 5*d* orbitals are stronger than those of the 3*d* orbitals due to their extended nature.

We will now discuss the low-energy spectral features observed in $\sigma(\omega)$ below 1.5 eV. As shown in Figs. 2(a) and 2(b), the $\sigma(\omega)$ of Sr_2RuO_4 and Sr_2RhO_4 exhibit Drude-like peaks, which are the characteristic optical response of a metallic state. The spectral weight of the Drude-like peak for Sr_2RhO_4 is one-third that of Sr_2RuO_4, which might be associated with the less metallic character of Sr_2RhO_4. Note that the Ru-O-Ru bond angle of Sr_2RuO_4 is 180°. In Sr_2RhO_4, the RhO_6 octahedra are rotated with respect to the *c* axis, so the *d* electron bands of Sr_2RhO_4 should become narrower. In addition, the number of the *d* electrons increases, so the electron correlation should increase.

In contrast to the metallic electrodynamics in Sr_2RuO_4 and Sr_2RhO_4, the $\sigma(\omega)$ of Sr_2IrO_4 shows an insulating behavior with an optical gap around 0.3 eV. The sharp spikes below 0.1 eV are due to optical phonon modes. Interestingly, Sr_2IrO_4 has a two-peak structure below 2 eV with a sharp peak near 0.5 eV. These spectral features below 2 eV are attributable to the splitting of the t_{2g} bands into the subbands below and above the E_F, as displayed schematically in Fig. 1(c). This splitting will lead to the *d*-*d* transition below the charge transfer excitations, as shown in Fig. 2(c).

However, the origin of the two-peak structure of Sr_2IrO_4 has not been determined. One possibility is the structural distortion in the electronic structure of Sr_2IrO_4. According to the recent angle-resolved photoemission spectroscopy result for Sr_2RhO_4, the mixing between the d_{xy} and $d_{x^2-y^2}$ bands driven by the rotation of the RhO_6 octahedra could lead to an almost fully occupied d_{xy} band with the remaining three electrons in $d_{yz/zx}$ bands,[21] and the $d_{yz/zx}$ bands in the layered structure are likely to have a one-dimensional nature.[22] Due to the structural similarity of Sr_2RhO_4 and Sr_2IrO_4, we postulate that similar effects hold for Sr_2IrO_4. Then, the quasi-one-dimensional $d_{yz/zx}$ bands might be subject to density wave instability, which could induce the insulating state of Sr_2IrO_4 and the fairly sharp peak in the $\sigma(\omega)$ near 0.5 eV. Indeed, Cao *et al.* suggested the possibility of a charge density wave in Sr_2IrO_4 based on its negative differential resistivity behavior.[10] However, the amount of structural distortion, i.e., the rotation of the metal-oxygen octahedra, is nearly the same in Sr_2RhO_4 and Sr_2IrO_4. Further systematic studies of the low energy peaks and a structural analysis of Sr_2IrO_4 are needed.

In summary, we investigated the electronic structures of Sr_2MO_4 (M=Ru, Rh, and Ir) systematically by measuring optical and XAS spectra. These spectroscopic studies demonstrated that these three compounds have similar interband transitions, indicating that their electronic structures are quite similar. The e_g orbital splittings were found to be very large, suggesting interesting roles of the electron-lattice coupling.

We thank J. S. Lee for valuable discussions. Experiments at PLS were supported in part by MOST and POSTECH. This work was financially supported by Creative Research Initiative Program (Functionally Integrated Oxide Heterostructure) of MOST/KOSEF, eSSC at POSTECH, and BK21. Y.S.L. was supported by the Soongsil University Research Fund.

---

*Email address: twnoh@snu.ac.kr

[1] J. G. Bednorz and K. A. Muller, Z. Phys. B: Condens. Matter **64**, 189 (1986).

[2] J. M. Tranquada, B. J. Sternlieb, J. D. Axe, Y. Nakamura, and S. Uchida, Nature (London) **375**, 561 (1995).

[3] Y. Tokura and N. Nagaosa, Science **288**, 462 (2000).

[4] Y. Maeno, H. Hashimoto, K. Yoshida, S. Nishizaki, T. Fujita, J. G. Bednorz, and F. Lichtenberg, Nature (London) **372**, 532 (1994).

[5] Y. Moritomo, T. Arima, and Y. Tokura, J. Phys. Soc. Jpn. **64**, 4117 (1995).

[6] J. H. Jung, K. H. Kim, D. J. Eom, T. W. Noh, E. J. Choi, J. Yu, Y. S. Kwon, and Y. Chung, Phys. Rev. B **55**, 15489 (1997).

[7] H.-J. Noh, S.-J. Oh, B.-G. Park, J.-H. Park, J.-Y. Kim, H.-D. Kim, T. Mizokawa, L. H. Tjeng, H.-J. Lin, C. T. Chen, S. Schuppler, S. Nakatsuji, H. Fukazawa, and Y. Maeno, Phys. Rev. B **72**, 052411 (2005).

[8] O. Friedt, M. Braden, G. Andre, P. Adelmann, S. Nakatsuji, and Y. Maeno, Phys. Rev. B **63**, 174432 (2001).

[9] M. Itoh, T. Shimura, Y. Inaguma, and Y. Morii, J. Solid State Chem. **118**, 206 (1995).

[10] G. Cao, J Bolivar, S. McCall, J. E. Crow, and R. P. Guertin, Phys. Rev. B **57**, R11039 (1998).

[11] I. Nagai and S. I. Ikeda (unpublished).

[12] S. Nakatsuji and Y. Maeno, Phys. Rev. B **62**, 6458 (2000).

[13] J. S. Lee, Y. S. Lee, T. W. Noh, K. Char, J. Park, S.-J. Oh, J.-H. Park, C. B. Eom, T. Takeda, and R. Kanno, Phys. Rev. B **64**, 245107 (2001).

[14] Y. S. Lee, J. S. Lee, T. W. Noh, D. Y. Byun, K. S. Yoo, K. Yamamura, and E. Takayama-Muromachi, Phys. Rev. B **67**, 113101 (2003).

[15] T. Arima, Y. Tokura, and J. B. Torrance, Phys. Rev. B **48**, 17006 (1993).

[16] J. Matsuno, Y. Okimoto, M. Kawasaki, and Y. Tokura, Phys. Rev. Lett. **95**, 176404 (2005).

[17] J. S. Lee, Y. S. Lee, T. W. Noh, S.-J. Oh, J. Yu, S. Nakatsuji, H. Fukazawa, and Y. Maeno, Phys. Rev. Lett. **89**, 257402 (2002).

[18] Z. Fang, N. Nagaosa, and K. Terakura, Phys. Rev. B **69**, 045116 (2004).

[19] J.-H. Park, T. Kimura, and Y. Tokura, Phys. Rev. B **58**, R13330 (1998).

[20] P. Kuiper, J. van Elp, D. E. Rice, D. J. Buttrey, H.-J. Lin, and C. T. Chen, Phys. Rev. B **57**, 1552 (1998).

[21] B. J. Kim *et al.*, Phys. Rev. Lett. (to be published).

[22] A. Damascelli, D. H. Lu, K. M. Shen, N. P. Armitage, F. Ronning, D. L. Feng, C. Kim, Z.-X. Shen, T. Kimura, Y. Tokura, Z. Q. Mao, and Y. Maeno, Phys. Rev. Lett. **85**, 5194 (2000).